Article

pubs.acs.org/Biomac

# Enhancing Enzyme Stability by Construction of Polymer–Enzyme Conjugate Micelles for Decontamination of Organophosphate Agents

Nisaraporn Suthiwangcharoen and Ramanathan Nagarajan*

Molecular Sciences and Engineering Team, Natick Soldier Research, Development and Engineering Center, 15 Kansas Street, Natick, Massachusetts 01760, United States

Supporting Information

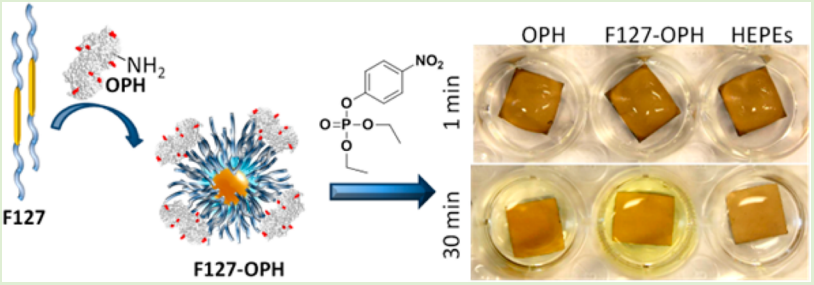


**ABSTRACT:** Enhancing the stability of enzymes under different working environments is essential if the potential of enzyme-based applications is to be realized for nanomedicine, sensing and molecular diagnostics, and chemical and biological decontamination. In this study, we focus on the enzyme, organophosphorus hydrolase (OPH), which has shown great promise for the nontoxic and noncorrosive decontamination of organophosphate agents (OPs) as well as for therapeutics as a catalytic bioscavanger against nerve gas poisoning. We describe a facile approach to stabilize OPH using covalent conjugation with the amphiphilic block copolymer, Pluronic F127, leading to the formation of F127-OPH conjugate micelles, with the OPH on the micelle corona. SDS-PAGE and MALDI-TOF confirmed the successful conjugation, and transmission electron microscopy (TEM) and dynamic light scattering (DLS) revealed ~100 nm size micelles. The conjugates showed significantly enhanced stability and higher activity compared to the unconjugated OPH when tested (i) in aqueous solutions at room temperature, (ii) in aqueous solutions at higher temperatures, (iii) after multiple freeze/thaw treatments, (iv) after lyophilization, and (v) in the presence of organic solvents. The F127-OPH conjugates also decontaminated paraoxon (introduced as a chemical agent simulant) on a polystyrene film surface and on a CARC (Chemical Agent Resistant Coating) test panel more rapidly and to a larger extent compared to free OPH. We speculate that, in the F127-OPH conjugates (both in the micellar form as well as in the unaggregated conjugate), the polypropylene oxide block of the copolymer interacts with the surface of the OPH and this confinement of the OPH reduces the potential for enzyme denaturation and provides robustness to OPH at different working environments. The use of such polymer–enzyme conjugate micelles with improved enzyme stability opens up new opportunities for numerous civilian and Warfighter applications.

## INTRODUCTION

Organophosphorus compounds (OPs) are highly toxic molecules that find applications as pesticides and insecticides, and they are also among the class of lethal chemical warfare agents. They can readily inactivate acetylcholinesterase (AChE), an enzyme that plays a critical role in the central nervous system, leading to paralysis and possibly death.[1,2] Over the last few decades, much effort has been devoted to developing methods to detect and inactivate the OPs, and one of the most promising is the use of the enzyme, organophosphorus hydrolase (OPH, also known as phosphotriesterase), to degrade the OPs.

OPH was originally isolated from soil bacteria and adapted to grow on organophosphates or the extra-chromosomal plasmids of the bacteria host that had been exposed to the pesticide.[3−5] The DNA sequencing performed on the opd cistron from *Pseudomonas diminuta* demonstrated the presence of an amino-terminal signal sequence, which was thought to control the cellular location (cytoplasmic vs membrane or outer surface associations) of the OPH activity in the native pseudomonad bacterium. The OPH produced from this gene was observed to be subject to variable processing depending upon the host strain. In the native pseudomonad and flavobacterium hosts, the enzyme was recovered in multiple molecular forms from cell-free lysates with molecular weights from 35000 to 39000 Da. The enzyme is a homodimer and the crystal structure of

Received: October 15, 2013
Revised: February 13, 2014
Published: February 24, 2014

  

OPH exhibited the overall fold of a distorted $(\beta/\alpha)_8$ or TIM-barrel.[6−8] The homodimer has approximately the size of 12 × 9 × 7 nm based on its crystal structure.

The catalytic activity of OPH was found to be associated with the protein encoded by the plasmid-borne gene (*opd*)[4,5] together with the two divalent metal ions in the active site of the OPH.[3] OPH easily loses its activity in the presence of chelating agents, but the activity can be recovered upon incubation with $Mn^{2+}$, $Co^{2+}$, $Cd^{2+}$, or $Ni^{2+}$.[3,9] Despite its high catalytic activity, the potential use of OPH is severely hindered because OPH has a low stability under different storage/working environments.[10] Current methods to stabilize OPH rely on immobilizations,[11−13] encapsulation,[10,13−15] or complexation with hydrogel,[16] fire-fighting foams,[17,18] and polyelectrolytes.[11,19] However, the challenge to develop a robust protocol which can preserve the OPH activity and conformation and stabilize the OPH under different working environments remains unfulfilled.

In this study, we describe our facile approach to stabilize OPH using covalent conjugation with amphiphilic block copolymers leading to the formation of block copolymer−OPH conjugates, which can exist as micelles even at low concentrations. The thermoresponsive Pluronic (trade name) triblock copolymer F127 (which is a symmetric triblock copolymer $PEO_{100}PPO_{64}PEO_{100}$, with hydrophilic polyethylene oxide, PEO in the ends and hydrophobic polypropylene oxide, PPO in the middle), was selected due to its environmental friendliness, biocompatibility, and chemical structure, which allows the enzyme conjugation to be easily implemented. Since the Pluronic family includes commercially available molecules with a wide range of molecular weights and block compositions, having the ability to spontaneously dissolve and self-assemble in water, it offers many potential candidates for conjugation to enzymes. Due to its amphiphilic nature, above its critical micelle concentration, the Pluronic block copolymer spontaneously forms micelles in aqueous solution with hydrophilic PEO shell or corona and hydrophobic PPO core. The covalent coupling of Pluronic micelles to proteins, antibodies, or polysaccharide is beginning to be explored[20,21] for applications in biomedicine, and this study is the first report, to the best of our knowledge, on the preparation and evaluation of Pluronic−OPH conjugate micelles for the decontamination application. We hypothesize that the F127-OPH conjugate micelles can prevent the OPH from aggregating to each other, thus, reducing the propensity for enzyme denaturation. The thermostability of F127 may provide robustness to the OPH at different working temperatures. The hydrophobic core can sequester the OPs having limited aqueous solubility and increase the interaction between the OPs and the OPH. The enhancement of enzyme activity following conjugation to the block copolymer compared to conjugation with the homopolymer PEG (polyethylene glycol) suggests that the propylene oxide (PPO) block of the Pluronic may indeed interact with the surface of OPH influencing the activity as well as stability. As a consequence of these beneficial physical-chemical features, we believe that the Pluronic−enzyme conjugation offers a general route to substantially increase the stability of the enzymes while also enhancing the enzymatic activity in comparison to the unconjugated enzyme as well as simple PEG conjugated enzymes.

## EXPERIMENTAL SECTION

**Materials.** The unconjugated enzyme, designated as Cys-$C_{30}$-mOPH, was kindly donated by the Olsen laboratory from MIT. This was prepared for research purposes by gene cloning into pQE9 expression vector and transferring into SG13009 cells for protein expression. This product differed from the wild type OPH through two important modifications. One was the replacement of five amino acids, Lys185Arg, Asp208Gly, His254Arg, Ile274Asn, and Arg319Ser (the numbers refer to the amino acid sequence in the wild-type OPH) and this modification was designated as mOPH. The other was the connection of a cysteine residue through a long spacer denoted as $C_{30}$, at the N-terminus of mOPH which is located at the opposite site of the OP binding pocket (enzyme active site). Both modifications were carried out in the Olsen laboratory by subcloning the Cys-C30 spacer gene into the pQE9 expression vector together with the mOPH gene. The $C_{30}$ spacer consists of nearly 320 amino acids (primary structure shown on Scheme S1) with no secondary structure and acts like a polyelectrolyte with high water solubility. Indeed the C30 addition to OPH was done to make OPH highly water-soluble overcoming any hydrophobicity. In the text below, we have referred to Cys-$C_{30}$-mOPH as simply OPH and this sample was used as the candidate for the block copolymer conjugation studies reported here.

Pluronic F127 (MW 12450 Da, 70% polyethylene oxide block and 64 propylene oxide units) was a gift from BASF. Succinic anhydride and methanol were purchased from Sigma Aldrich. 4-Dimethylaminopyridine (DMAP) and *N*-hydroxysuccinimide (NHS) were purchased from Alfa Aesar. Triethylamine, 1,4-dioxane, and dichloromethane were purchased from Sigma Aldrich. 1-Ethyl-3-(3-dimethylaminopropyl)carbodiimide (EDC) was purchased from ACROS Chemical Company. Paraoxon (*O*,*O*-diethyl *O*-(4-nitrophenyl) phosphate) was purchased from Sigma Aldrich (EC Number 206−221−0). HEPEs buffer (50 mM, pH 8) containing 0.1 mM $CoCl_2$ and 50 mM NaCl was used throughout the experiment unless specify otherwise.

*Synthesis of Carboxylated-Pluronic F127 (F127-COOH).* The synthesis was conducted following previous reports.[20] Briefly, F127 (6.3 g; 1 mmol OH) and DMAP (122.17 mg; 1 mmol) were dissolved in 1,4-dioxane (15 mL) with the presence of TEA (139 μL) and allowed to stir under $N_2$ for 30 min. Succinic anhydride solution (125 mg in 5 mL 1,4-dioxane) was then added dropwise to the Pluronic solution while stirring. The solution mixture was allowed to stir at room temperature for 24 h. The excess 1,4-dioxane was removed by rotary evaporation, and the remaining samples were precipitated three times in cold diethyl ether while stirring. The precipitate was dried under vacuum overnight at room temperature to give the white powder of F127-COOH. The presence of COOH was analyzed using FT-IR and $^1$H NMR (Figure S1).

*Synthesis of NHS-Terminated F127 (F127-NHS).* In this step, the carboxyl-terminated F127 was activated with NHS. Briefly, F127-COOH (500 mg; 0.08 mmol) and EDC (77 mg; 0.4 mmol) were dissolved in 5 mL of dichloromethane in a round-bottom flask. After stirring the mixture for 30 min, NHS (46 mg, 0.4 mmol) was added, and the solution mixture was left stirring at room temperature for 24 h. Next day, the solution mixture was precipitated three times in cold diethyl ether. The precipitate was further dried under vacuum overnight at room temperature to give the white powder of F127-NHS. The presence of NHS was confirmed using FT-IR and H NMR (Figure S1).

*OPH attachment to F127.* The strategy for attaching OPH to F127 was adapted from previous literature.[21−25] Briefly, OPH solution (1 mL of 0.2 mg·mL$^{-1}$) was added dropwise into the F127-NHS solution (1 mL of 40 mg·mL$^{-1}$) while stirring. The mass ratio of F127 to OPH was 200 and the mole ratio was approximately 1000, and such overwhelming excess was used to improve the probability of OPH conjugation. The reaction mixture was allowed to stir at 4 °C for 4 h. At this temperature, the F127 block copolymer and its end functionalized forms do not exist in micellar state (as confirmed by dynamic light scattering, Figure S2) and therefore the conjugation involved reaction between unaggregated F127-NHS and the OPH.

**Scheme 1. Schematic Representation of the Conjugation of OPH to Pluronic F127 to Create F127-OPH Conjugate Micelles**[a]

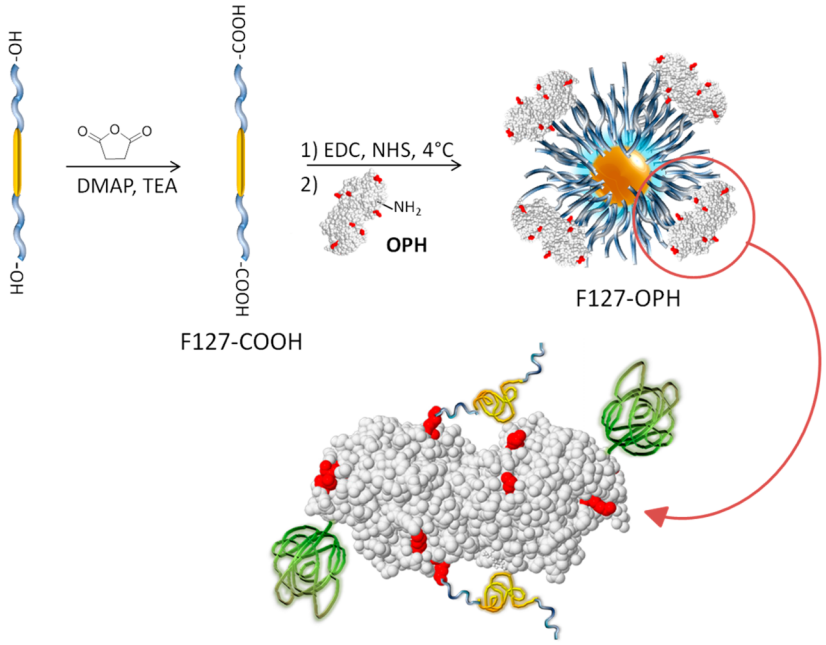


[a]F127 was first activated to introduce the carboxyl function at the end. OPH was then covalently attached through the EDC/NHS coupling reaction. The detailed view of the OPH dimer used shows the C30 modification (polyelectrolyte like polypeptide chain) on each monomer to increase the aqueous solubility. Also indicated are some of the lysine residues accessible for conjugation to F127-NHS. Of the two F127 molecules conjugated to each dimeric OPH, one or both could be inserted into the micelle core. The polypropylene oxide block from the conjugate will also have favorable interactions with the hydrophobic surface patches on OPH.

Following the conjugation reaction, the samples were centrifuged between 8000 and 16000*g* for 20 min to remove any unconjugated OPH and the ester byproduct, followed by resuspension in buffer. This step was repeated at least three times. The purification process was monitored by sodium dodecyl sulfate polyacrylamide gel electrophoresis (SDS-PAGE) using NuPAGE Novex 12% Bis-Tris Gel (Molecular Probes, Invitrogen) with MOPS running buffer (Invitrogen). The gel was stained with Coomassie Blue prior to visualization. Typically, there was no indication of any measurable presence of free OPH in the supernatant. When no more free OPH was detected, the reaction mixture was lyophilized and kept at −20 °C.

The amount of OPH attached to F127 was determined using standard Coomassie (Bradford) Protein Assay (Pierce, Rockford, IL). OPH solutions with known concentrations were used as standards. Molecular weight of the conjugate was determined using MALDI-TOF mass spectrometer. Samples were prepared by plate spotting of the samples, which were premixed with a sinapinic acid matrix. The unconjugated OPH and F127 were used as reference samples.

**Instruments.** $^1$H NMR was acquired on a Bruker ARX 500 MHz spectrometer. Infrared spectroscopy was recorded on a Perkin-Elmer Spectrum One Fourier Transform IR (FTIR), equipped with the ATR accessory. The hydrodynamic diameter and size distributions were measured with dynamic light scattering (DLS, Zetasizer Nano ZS, Malvern Instruments). The deconvolution was accomplished using a non-negatively constrained least-squares fitting algorithm. The measurements were taken at 90° scattering angle. Static light scattering was also done using the same instrument to obtain the absolute molecular weight of aggregates. The unconjugated OPH was used as a reference sample.

**Circular Dichroism (CD).** The CD measurements were made using the circular dichroism spectrophotometer (Aviv Biomedical, Inc., Lakewood, NJ) with a path length of 1 mm. Measurements were carried out on OPH or F127-OPH in diluted HEPEs buffer solution (pH 8), keeping the enyme concentration at 100 $\mu g \cdot mL^{-1}$. Far-UV CD spectra were measured from 190 to 240 at 1 nm intervals. Three scans were accumulated and averaged for each spectrum after the background of diluted blank buffer was subtracted.

**TEM Analysis.** TEM images were obtained on JEOL 2010 TEM equipped with a LaB6 (lanthanum hexaboride) filament, operated at 200 KeV with GIF 2001 spectrometer and 1 megapixel CCD camera. For sample preparation, 10 $\mu$L of each sample was dropped on a copper grid and allowed to evaporate overnight. Then, 10 $\mu$L of phosphotungstic acid (PTA) solution (2% w/v) was added to the grid. After 2 min, the solution was drawn off from the edge of the grid with filter paper, and the grid was allowed to air-dry prior to the analysis.

**Enzymatic Activity and Stability Assay.** The activity of F127-OPH conjugate in the hydrolysis of paraoxon was evaluated in HEPEs buffer (pH 8) with the presence of $CoCl_2$ and NaCl. Briefly, an aqueous solution of paraoxon containing 10% v/v methanol was added to OPH or F127-OPH with the same enzyme concentrations to give the final concentrations of 0.075 $\mu$g/mL of OPH and 0.1 mM paraoxon. The activity levels were measured by monitoring the release of p-nitrophenol product spectrophotometrically at 405 nm for 10 min using Eon BioTek Microplate Spectrophotometer. The concentration of *p*-nitrophenol was determined based on the standard calibration curve.

The kinetic parameters for OPH and F127-OPH were obtained by measuring initial hydrolysis rate of different paraoxon concentrations, keeping a constant enzyme concentration. The kinetic constants were determined by fitting the data to Lineweaver−Burk reciprocal plot. All assays were performed in triplicate.

For the stability assay, OPH and F127-OPH solutions with the same OPH concentrations were both incubated at 70 °C. Samples were taken out at different time intervals and immediately stored on ice. The enzymatic activity was measured by the hydrolysis of paraoxon using the aforementioned procedure. All of the assays were performed at least in triplicate, and the average was reported.

**Decontamination of Chemical Agent Resistant Coating (CARC) Surface.** Paraoxon solution in methanol (25 $\mu$L; 0.8 mM) was added to the surface of the CARC. The methanol was allowed to completely evaporate. Then the OPH or F127-OPH solution (200 $\mu$L; enzyme concentration of 2 $\mu g \cdot mL^{-1}$ in both) was gently added onto the CARC surface. The reaction was quenched after specified times with methanol, and the extraction was allowed to proceed for another

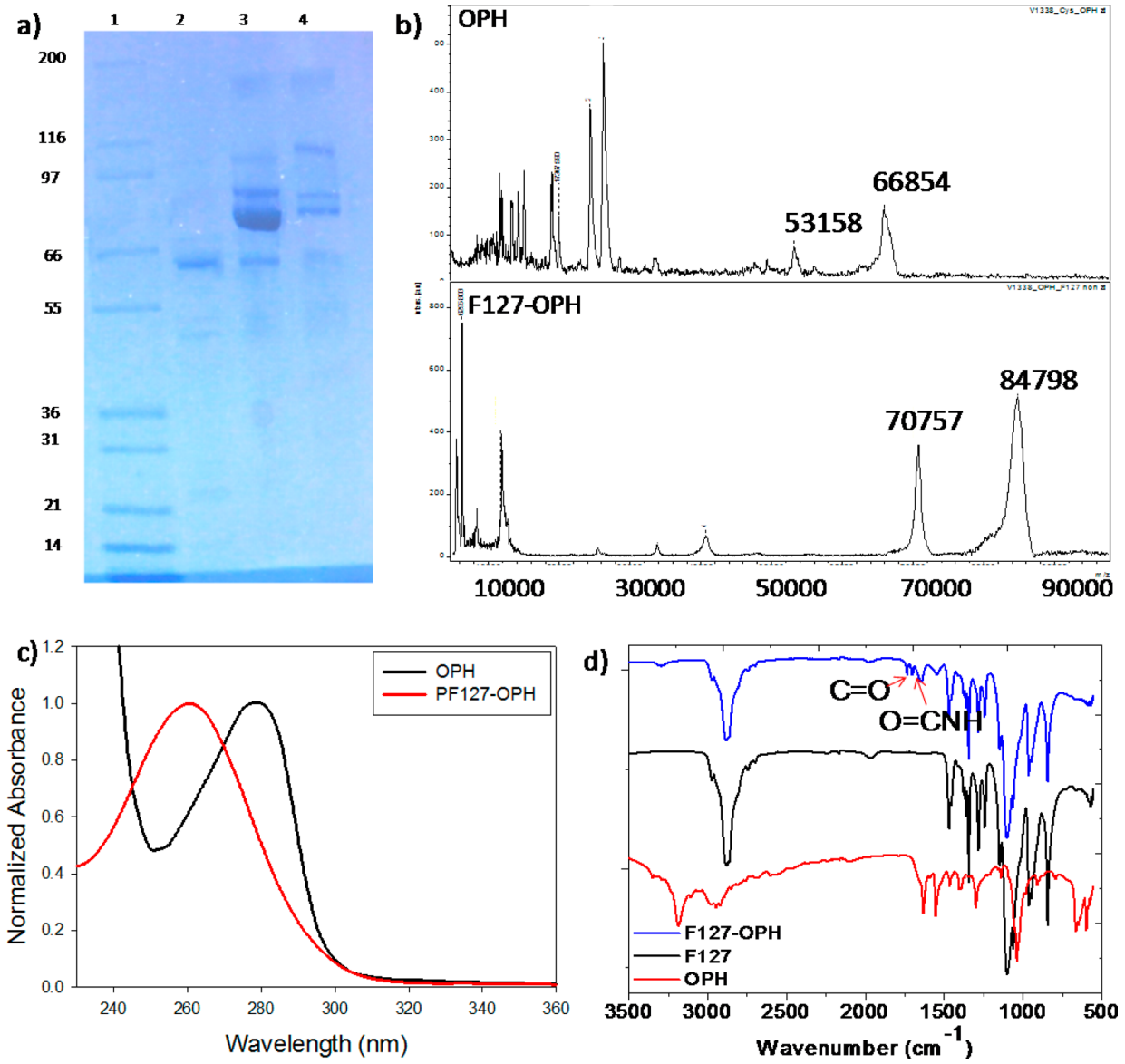


**Figure 1.** (a) SDS-PAGE of (1) molecular weight markers, (2) unconjugated OPH, (3) F127-OPH (crude), and (4) F127-OPH (purified). (b) MALDI-TOF of unconjugated OPH and F127-OPH. The increase in molecular weight after a conjugation confirmed a successful conjugation of the OPH to F127 and suggested that there was approximately one Pluronic molecule per OPH monomer. (c) UV−vis spectra of OPH and F127-OPH. A slight blue-shift after the conjugation was observed indicating that there may be a change of the microenvironment polarity to a more apolar environment around the tryptophan and/or tyrosine residues of OPH. (d) FTIR spectra of OPH, F127, and F127-OPH. The new peaks at 1732 and 1689 $cm^{-1}$ (red arrows) which are attributed to the carbonyl stretching vibration and the typical bands of amide carbonyl (O═CNH) group, are clearly observed, indicating that the conjugation occurred via the formation of amide bonds between OPH and F127-COOH.

hour before the measurement. The decontamination and extraction efficiency were determined using the $\varepsilon_{405}$ = 16241 $M^{-1}$ $cm^{-1}$ when a 1:1 mixture of methanol and HEPEs buffer was used as a medium.

## RESULTS AND DISCUSSION

**F127-OPH Conjugation.** The preparation of the F127-OPH can be achieved via the chemical conjugation between OPH and the hydrophilic ends of the F127 block copolymer. As depicted in Scheme 1, since the Pluronic is chemically inert, it was first activated with succinic anhydride to introduce carboxyl groups at the termini of F127 (F127-COOH). The $^1H$ NMR spectrum of the F127-COOH showed a prominent peak at ∼2.6 ppm, corresponding to the protons of the new methylene groups obtained from succinic anhydride (Figure S1). The NHS ester was subsequently introduced to the Pluronic via a common EDC/NHS reaction. The excess EDC/NHS was removed prior to the reaction with the OPH to prevent the reaction between the enzyme itself. The F127-NHS was then reacted with the lysine residues on the OPH, leading to the formation of F127-OPH conjugate. The conjugation was performed at 4 °C and since at this condition, the end functionalized F127 does not form micelles but remains unaggregated (as confirmed by dynamic light scattering, Figure S2), the conjugation reaction occurs between unaggregated F127 and the OPH. Since each OPH monomer contains eight lysine residues,[22] multiple site conjugations may occur on the monomer and result in an abundance of polymer on the surface of the OPH that subsequently could deactivate the enzyme. To suppress this effect, the pH of the reaction mixture was maintained at ∼7.8 to keep the $-NH_2$ in the unprotonated


dx.doi.org/10.1021/bm401531d | *Biomacromolecules* 2014, 15, 1142−1152

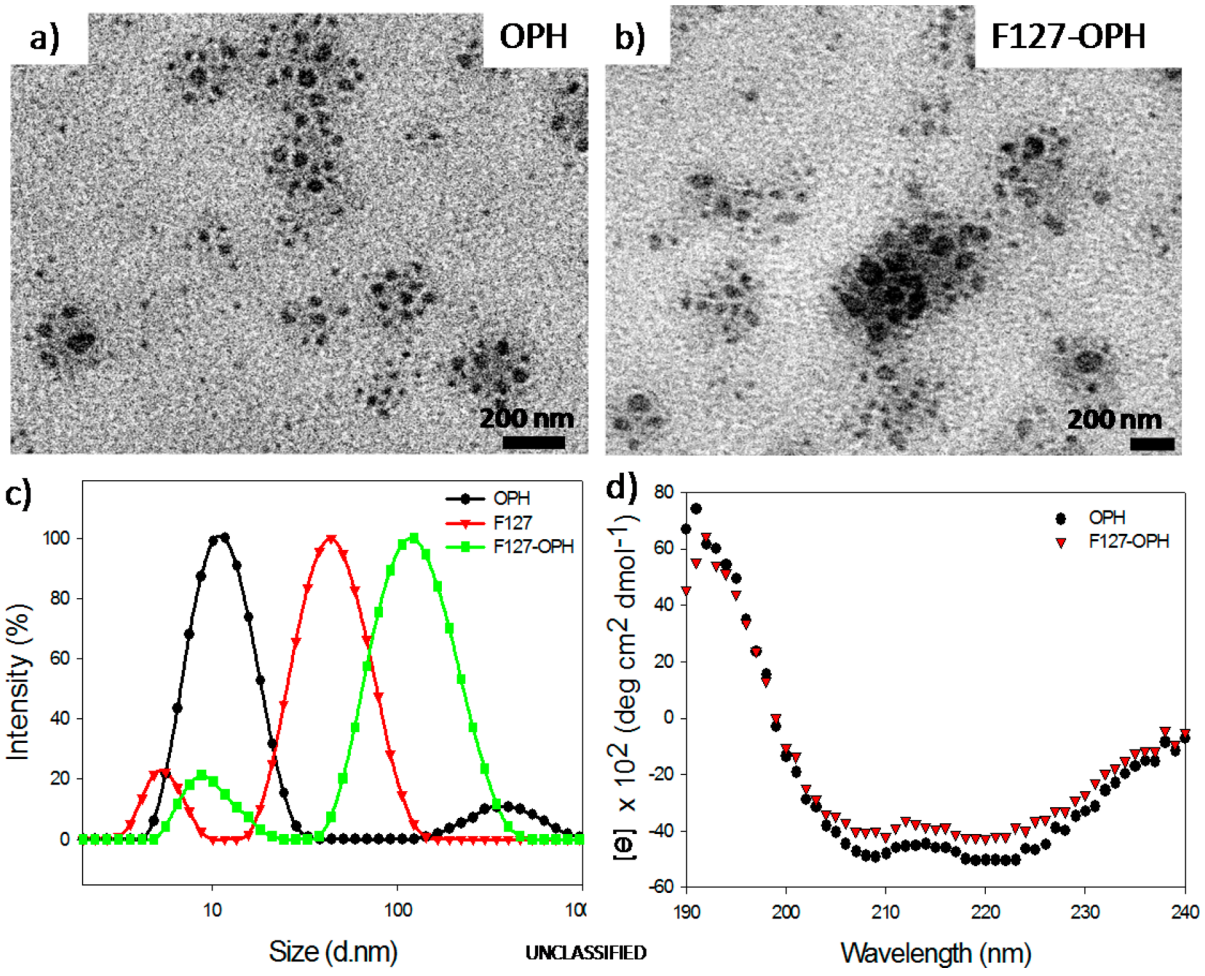


**Figure 2.** (a, b) Transmission electron microscopy images of F127 micelles and F127-OPH micelles, respectively. The samples were stained with phosphotungstic acid prior to the analysis. (c) Dynamic light scattering of OPH, F127, and F127-OPH micelles. The average hydrodynamic size of the conjugate micelles was shown to increase to about 100 nm in diameter. (d) Circular dichroism spectra of OPH and F127-OPH. Both spectra exhibit two minima at 209 and 222 nm, indicating that the conjugation did not significantly affect the secondary structure of the OPH.

form and to allow the reaction to preferably take place with the most fully solvent exposed $\varepsilon$-amine groups (Lys175 and Lys294).[22] It is possible that the other two lysines (Lys77 and Lys339), which are partially exposed to the solvent, may still be able to conjugate with the polymer.

After extensive purification to remove any unconjugated OPH by centrifugation, the conjugation was confirmed using SDS-PAGE, showing the molecular weight of the OPH increasing from 66 kDa to about 80−100 kDa (Figure 1a). The results were further confirmed by MALDI-TOF (where the molecular weight cut off was at 100 kDa). The increase in apparent molecular mass as determined by both SDS-PAGE and MALDI suggested that there was approximately one Pluronic molecule per OPH monomer (Figure 1a,b). The total amount of enzyme in F127-OPH purified product was estimated by the Coomassie (Bradford) Protein Assay to be 162 $\mu g \cdot mL^{-1}$ indicating that nearly 80% of the enzyme that was used in the reaction was successfully conjugated.

A slight blue-shift after the conjugation was observed in the UV−vis spectrum indicating that there may be a change of the microenvironment polarity to a more apolar environment around the tryptophan and/or tyrosine residues of OPH (Figure 1c).[26,27] This could be due to the interactions of the polypropylene oxide block of the block copolymer in the conjugate with the hydrophobic surface patches of OPH. Further analysis of the F127-OPH conjugate was performed using FTIR (Figure 1d). F127 showed three major peaks at 960, 1092, and 1279 $cm^{-1}$, while the unconjugated OPH showed major peaks at 1551, 1625, 2944, and 3182 $cm^{-1}$. When comparing the FTIR spectrum of Pluronic before and after conjugation, the new peaks at 1732 and 1689 $cm^{-1}$, which are attributed to the carbonyl stretching vibration and the typical bands of amide carbonyl ($O$ = CNH) group, are clearly observed, indicating that the conjugation occurred via the formation of amide bonds between OPH and F127-COOH.

**Characterization of F127-OPH Conjugates in Solution.** The F127-OPH conjugate solution includes F127-OPH conjugate molecules as well as free F127-NHS molecules, since a large excess of F127-NHS was used in the conjugation. Because of the amphiphilic character of the block copolymer, F127-NHS forms micelles (just as F127 and F127-COOH) with polypropylene oxide core and polyethylene oxide corona.[28] The F127-OPH molecules are expected to be included in these self-assembled structures. Transmission electron microscopy (TEM), dynamic light scattering (DLS), and static light scattering (SLS) were used to characterize the morphology and size distribution of the F127-OPH conjugate micelles. After staining with phosphotungstic acid solution,


dx.doi.org/10.1021/bm401531d | *Biomacromolecules* 2014, 15, 1142−1152

spherical micelles of the pure F127 with a diameter of about 50 nm were observed (Figure 2a) in the TEM. Upon conjugation with OPH, the size of the micelles increases to about 100 nm in diameter, with a narrow size distribution (Figure 2b) as seen by the TEM and also by DLS (Figure 2c).

The secondary structure of the OPH after a conjugation was evaluated using circular dichroism (CD). Unconjugated OPH exhibits two strong minima of $\alpha$-helix content at 209 and 222 nm (Figure 2d).[13] This clearly shows that the secondary conformation of OPH is not disturbed by the attachment of the $C_{30}$ polyelectrolyte chain which has been introduced to make the enzyme more water soluble. The F127-OPH conjugate shows slightly less negative peaks, yet both minima at 209 and 222 nm still persist, indicating that the conjugation does not significantly affect the secondary structure of the OPH.

The particle size from DLS analysis (Figure 2c) reveals results similar to that from TEM. The DLS results for the unconjugated OPH suggest an hydrodynamic diameter in the range of 10 to 20 nm. As mentioned previously, the size of the OPH dimer estimated from its crystal structure was about 12 × 9 × 7 nm. One would have to add to this the contributions from the $C_{30}$ modification made on each OPH monomer and the resulting diameter would be comparable to what is seen from the DLS. The DLS data for the unconjugated F127 micelles indicate a diameter of about 50 nm. This is similar to the result from the TEM and is also comparable to the DLS data obtained for F127-COOH (Figure S2). The DLS data for F127-OPH shows a main population of F127-OPH micelles at about 120 nm. If one adds the size of OPH to the unconjugated F127 micelles, one would get a diameter of about 90 nm for F127-OPH. Clearly, the incorporation of F127-OPH also changes the aggregation characteristics of F127, presumably by extending the coronal region (since the PPO core must remain compact because of the hydrophobic nature of the domain). This is reasonable since an extended coronal region will correspond to increased dilution of the PEO segments in the corona in order to allow the penetration of the $C_{30}$ hydrophilic attachment on the OPH. The DLS data for F127-OPH also shows a small population at ~10 nm. This may belong to some residual free OPH (the free OPH was mostly removed by the centrifugation method as indicated on the SDS-PAGE) since the intensity plots of DLS can capture even very small concentrations of scattering particles.

The size of F127-OPH micelles was also determined from static light scattering (Figure 3). The intensity versus concentration data can be used to estimate the absolute molecular weight of the micelles in solution as well as the second virial coefficient representing the nature of interactions between the micelles. The data are plotted in the form of the classical Debye plot given by the relation

$$\frac{KC}{R_\theta}P(\theta) = \frac{1}{M} + 2A_2C$$

where $K$ is the optical constant of the instrument, $C$ is the concentration of the solution, $R_\theta$ is the Rayleigh ratio directly connected to the measured scattering light intensity, $P$ is the shape or form factor (taken to be that for a spherical particle), $M$ is the molecular weight, and $A_2$ is the second virial coefficient.

From Figure 3, we estimate the absolute molecular weight to be approximately 1500 kDa. Recognizing that F127 has a molecular weight of about 13 kDa and the molecular weight of F127-OPH conjugate in the dimeric protein form is about 170 kDa (twice the value observed from the MALDI in Figure 1b), the SLS data points to a multimolecular aggregate incorporating one or more F127-OPH conjugate molecule and a large number of unconjugated F127 molecules. The slope of the Debye plot is positive indicating that the second virial coefficient $A_2$ is positive. A positive second virial coefficient implies that the particles repel each other and prefer to be interacting with the solvent rather than with each other. This is consistent with the use of OPH, which has strongly hydrophilic $C_{30}$ chains attached to it, with the polyelectrolyte character of the $C_{30}$ chain dominating over any surface hydrophobicity of the native OPH.

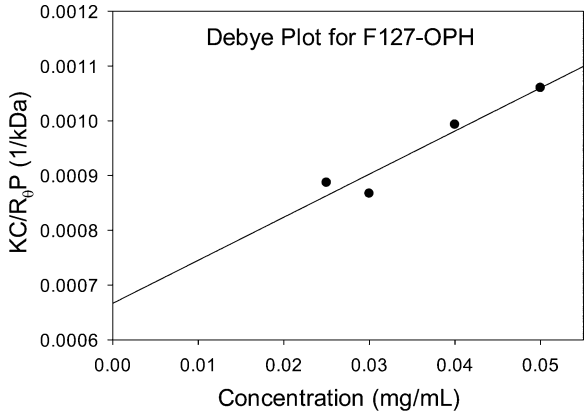


**Figure 3.** Static light scattering plot for F127-OPH. The intercept is used to calculate the absolute molecular weight of the micelles and the slope provides the second virial coefficient representing interactions between micelles.

The increased size of the F127-OPH micelle compared to F127 micelles observed from DLS, the positive second virial coefficient representing stronger micelle-water affinity over micelle−micelle affinity observed from SLS, the expectation to finding OPH in the aqueous domain because of the presence of the polyelectrolyte like $C_{30}$ attachment are all supportive of the concept that the OPH is located on the corona surface of the micelle, in spite of the hydrophobic patches on the surface of the native OPH. Indeed, native OPH shows the tendency to rapidly aggregate (data not shown here), indicating the attractions arising from the contacts between the surface hydrophobic patches. We speculate that the polypropylene oxide blocks of the F127 conjugated to OPH may protect these hydrophobic regions, which are forced to exist in the aqueous domain because of the water solubility provided by the $C_{30}$ modification.

**Enzymatic Activity of the F127-OPH Micelles.** It has been reported that the enzyme conjugation or immobilization can result in a decrease in the enzymatic activity.[22] In that study, OPH was conjugated with linear and branched methyl-PEO$_n$-NHS esters (of molecular mass from 333 to 2420 Da). In all cases, the PEGylated OPH displayed a decreased maximal catalytic rate, though substantial activity was still retained. Therefore, PEGylation as a method to improve stability was found to reduce the activity. In our work, to investigate whether the OPH is still active after conjugating to F127 micelles, the activity of OPH and F127-OPH micelles was tested against paraoxon, a V-type neurotoxin stimulant. Both OPH and F127-OPH micelles have shown to catalyze the hydrolysis of paraoxon and produce *p*-nitrophenol, a fluorogenic product that can be easily detected using a spectrophotometer. Using

OPH solution as a blank spectrum, the peak at 280 nm was attributed to the paraoxon molecules. The addition of OPH leads to a decrease of the peak at 280 nm and a simultaneous increase of the peak at 405 nm, which is attributed to the *p*-nitrophenol molecules, with an isosbestic point at 310 nm (Figure S3). Similar results were observed with a higher hydrolytic rate when F127-OPH micelles were used, implying that the enzymatic activity after conjugating was preserved. The unmodified OPH and F127-OPH micelles displayed Michaelis–Menten kinetics (Table 1), with $k_{cat}$ values of the conjugate micelles being about 1.5 times higher than that of the unmodified OPH (Figure S4). Since paraoxon (0.1 mM) was relatively soluble in an aqueous solution, no change in the $K_m$ value was observed. However, the increase in $k_{cat}$ clearly suggests that F127-OPH micelles can be used as effective decontamination agents.

**Table 1. Kinetic Parameters of Unmodified OPH and F127-OPH Micelles**[a]

| sample | $K_m$ (mM) | $k_{cat}/K_m$ ($s^{-1}$ $M^{-1}$) |
|---|---|---|
| OPH | 0.0274 ± 0.007 | 1.02E6 ± 2.2E5 |
| F127-OPH | 0.0270 ± 0.003 | 1.49E6 ± 1.3E5 |

[a]Values represent means of triplicate experimental data, as indicated by the standard deviation (mean ± st dev).

We rationalized that the increase in the catalytic activity of the OPH after conjugation maybe attributed to multiple reasons: (i) the local concentration of enzyme is increased;[29] (ii) the substrate, organophosphate agent, can be solubilized in the micelle core increasing its proximity to the enzyme; (iii) the crowding effect[30] due to higher macromolecular concentration in the proximity of the enzyme; and (iv) the protection of the active region of the enzyme by the polypropylene oxide block of the F127 conjugated to the enzyme. Reason (i) may not be important because the overall concentration of the enzyme used in the activity studies was kept very small. Reason (ii) may not be important in this case, because of the relatively appreciable aqueous solubility of the substrate paraoxon. The crowding effect could play a role, but such crowding effect, which would have been relevant even for the case of PEGylated OPH discussed above,[22] resulted in a decrease in the enzyme activity rather than an increase. Therefore, we speculate that reason (iv) based on possible interactions of the hydrophobic polypropylene oxide block of the F127 molecule conjugated to OPH with the hydrophobic surface domains on the OPH surface that are close to ligand pockets may be responsible for providing some enhancement in activity. Compared to free F127 molecules, the conjugated F127 molecules may allow for this interaction between PPO and OPH to occur more effectively. Support for such interactions was provided by the observed spectral shift shown in Figure 1c.

Since OPH can potentially be used as prophylactic against acute OP poisoning, we evaluated the activity of the F127-OPH-micelles at 25 and 37 °C, using paraoxon in a liquid formulation (shown in Figure 4a with marking "l") and also using dried paraoxon on a surface (shown in Figure 4a with the marking "f"). Against the liquid formulation, in comparison to the unconjugated OPH, the enzymatic activity against paraoxon was shown to be ∼30% higher when F127-OPH was used. When the temperature was raised to 37 °C, the activity of F127-OPH increased while no significant change in the activity of OPH was observed. To measure the ability of F127-OPH micelles to inactivate dried paraoxon on a flat surface, a solution of paraoxon in methanol was added onto a polystyrene substrate, and the solvent was allowed to completely evaporate at room temperature. Once the thin film of paraoxon was created, the OPH or F127-OPH solution at the same enzyme concentration was added directly to the dried paraoxon film, and the hydrolytic activity was measured. As shown in Figure 4a, it was found that F127-OPH exhibits a ∼20% increase in activity when the dried paraoxon coating on a solid surface was used at 25 °C. When the temperature was raised to 37 °C, a 10% increase in activity was observed in comparison to that at 25 °C. While the activity of the unmodified OPH was shown to be similar under both liquid and dried paraoxon, the F127-OPH exhibits about ∼1.5-fold enhancement in activity. This observation clearly suggests the great potential of using F127-OPH micelles as an effective candidate for decontamination agents.

**Stability of the F127-OPH Micelles.** To investigate the thermal stability of the F127-OPH conjugates at elevated temperature, the samples along with the unconjugated OPH were incubated at 70 °C (a typical condition used in the literature to allow OPH or other proteins to be denatured and aggregated[13]), and the activity was measured at different time intervals. As depicted in Figure 4b, OPH completely lost its activity after 10 min of the incubation time, whereas the activity of the F127-OPH was retained to about 37%. A significant decrease in activity for F127-OPH was observed during the first 10 min of the incubation time, then the activity only slowly dropped. After 120 min of the incubation time, the activity of the F127-OPH still remained at about 15%.

The enhanced freeze–thaw stability was demonstrated in Figure 4c. After five freeze–thaw cycles, the F127-OPH retains more than 80% activity while the unconjugated OPH showed more than 50% decrease in activity after the second cycle and completely lost its activity after the fourth cycle. The half-life data for OPH and F127-OPH under different storage conditions are summarized in Table 2.

We believe that the conjugation between OPH and F127 and the presence of micelles might prevent conformational transitions of OPH at high temperature or during the freeze–thaw cycles as the micelles offers benign microenvironment[31] to assist the conformational preservation of OPH; hence, the F127-OPH micelles can maintain the thermal stability of the OPH against the unfolding transition at the transition temperature, comparing to that of the unconjugated enzyme in the solution. In addition, it was previously shown that the change in temperature induces the aggregation of the enzyme, primarily due to the loss of tertiary structure of enzyme.[32,33] By introducing the use of conjugate micelles, the thermal inactivation of OPH resulting from the aggregation effect could be minimized.

We further evaluated the stability of OPH at low concentrations. As is well-known, many enzymes are prone to degradation at a low concentration. The activity drop of unconjugated OPH (0.5 ug/mL) was observed within the first two hours when storing at 4 and 25 °C, and a complete loss of original activity of OPH was observed after 72 h of storage time (Figure 4d,e). Upon the conjugation with F127, the activity of the conjugated OPH remained unchanged throughout 3 months under the same conditions, indicating that the micelles can prolong the shelf life of the OPH (Figure 4f). To increase the long-term stability and ease of handling and transporting, the freeze-drying technique was applied to the F127-OPH

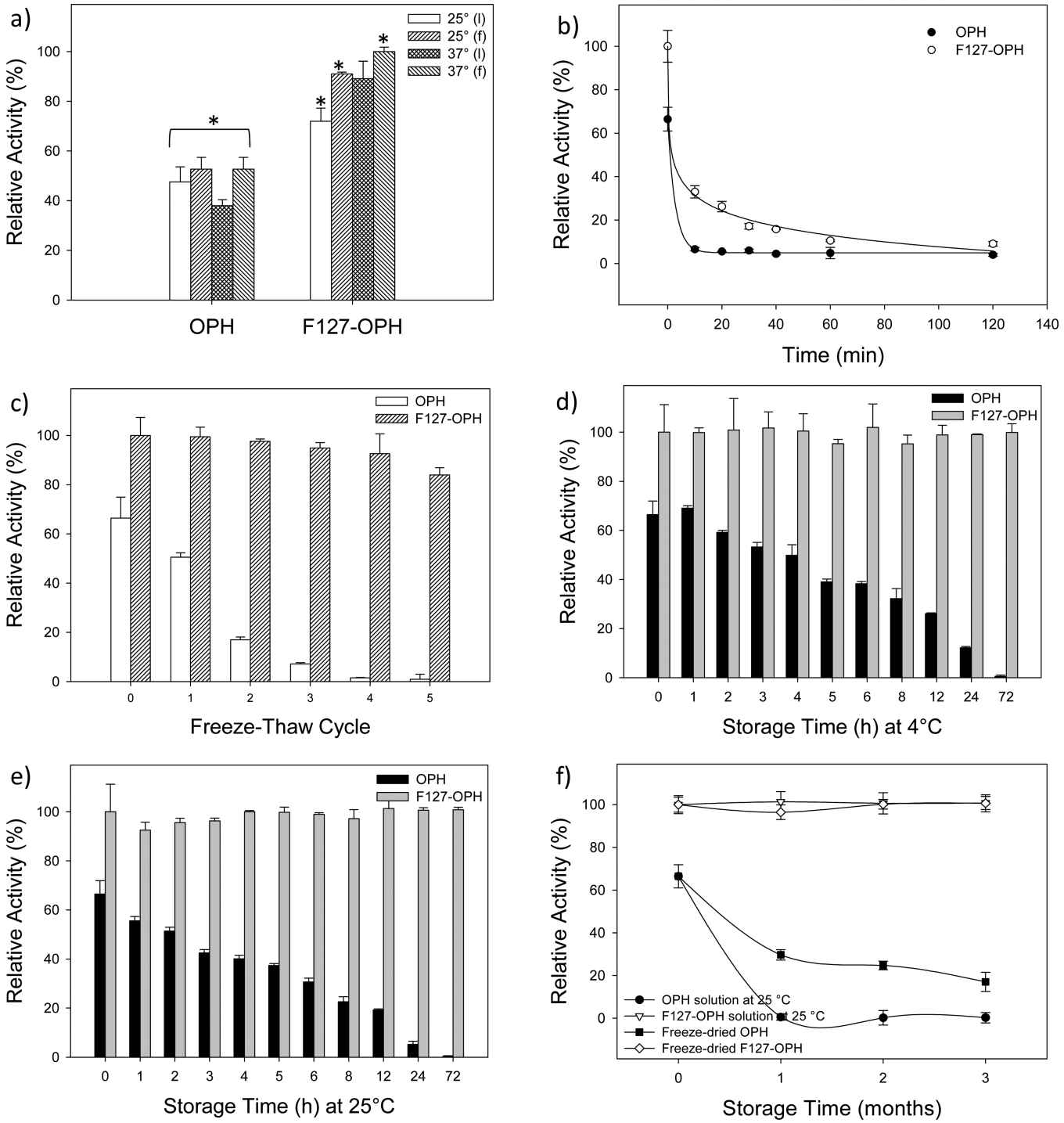


**Figure 4.** Relative activities of OPH and F127-OPH (a) in the presence of liquid and dried paraoxon at 25 and 37 °C (*$p$-value < 0.05 vs F127-OPH control), (b) after incubation at 70 °C, (c) after five freeze−thaw cycles, (d) after storing at 4 °C in a solution form, (e) after storing at 25 °C in a solution form, and (f) after lyophilization and a 3-month storage. For all the data, 0.075 ug/mL enzyme concentration and 0.1 mM paraoxon were used.

micelles, and the OPH activity of the powder was determined periodically. As illustrated in Figure 4f, the unconjugated OPH suffers severe activity drops after freeze-drying with less than 45% of its original activity, and the activity slowly drops through the 3 months while storing at 4 °C in a dry formulation. In contrast, the activity of freeze-dried F127-OPH was virtually unchanged throughout 3 months. A great long-term stability of this formulation offers promising benefits in cost effectiveness, sample handling, and other practical applications.

While many OP compounds are well solubilized in various organic solvents, the OPH molecule is inactivated in the presence of organic solvents. Here, the enhancement in the OPH stability with the presence of organic solvents was demonstrated by exposing both unconjugated OPH and F127-OPH conjugates in different organic/aqueous volume ratios. Methanol and dimethylsulfoxide (DMSO) were employed as


dx.doi.org/10.1021/bm401531d | *Biomacromolecules* 2014, 15, 1142−1152

**Table 2. Half-Life ($h$) of OPH and F127-OPH under Different Storage Conditions[a]**

| storage condition | OPH | F127-OPH |
|---|---|---|
| incubation at 70 °C | 0.05 | 0.1 |
| 4 °C in a solution | 10.6 | nd |
| 25 °C in a solution | 2.2 | nd |
| lyophilization | 626.9 | nd |
| 10% (v/v) methanol | 4.7 | nd |
| 10% (v/v) DMSO | 5.5 | nd |

[a]"nd" indicates that the half-life was not determined because the enzyme activity remained unaffected over the long duration of the experiments and the experiments were not extended to allow the determination of a half-life.

polar protic and aprotic solvents, respectively. As depicted in Figure 5, although the activities of both OPH and F127-OPH decrease as the volumetric fractions of the organic solvents increase, the F127-OPH retained higher enzymatic activity in every solvent ratio in the presence of either solvent. In addition, the F127-OPH was shown to be stable in the presence of 10% (v/v) organic solvent even after 25-day storage (Figure 5c,d). We believe that the presence of the micelles and also the possible protection of OPH afforded by the PPO block of the F127 block copolymer could prevent some parts of the OPH from being denatured by the organic solvents, which are known to disrupt the intramolecular interactions, such as hydrogen bonds of the proteins.[34]

**Decontamination of Chemical Agent Resistant Coating (CARC) Surface.** The use of F127-OPH as an effective decontamination agent was demonstrated on the chemical agent resistant coating (CARC) surface (Figure 6a). Briefly, the CARC surface was first contaminated with a paraxon solution in methanol. After the complete evaporation of methanol, the unconjugated OPH or F127-OPH solution was added to the contaminated surface, and the decontamination efficiency was determined periodically with a methanol quenching and extraction. Within 15 min of decontamination, the OPH and F127-OPH exhibited ~30 and 60% decontamination efficiency, respectively, and reached up to 60 and 90% after 1 h (Figure 6b,c). Although the contaminated CARC surfaces can be treated with the unconjugated OPH solution, the unconjugated enzyme itself is not stable enough for a wide-area or long-term decontamination, since the stability of the unconjugated OPH was shown to decrease at room temperature. The control studies using 1:1 HEPEs/methanol showed ~96% extraction of paraoxon while no decontamination was observed (see Supporting Information, Table S1), indicating that the solvents are capable of removing the paraoxon from the CARC surface but the contaminant would remain as a toxic waste in the absence of enzymatic reactive decontamination. The relatively

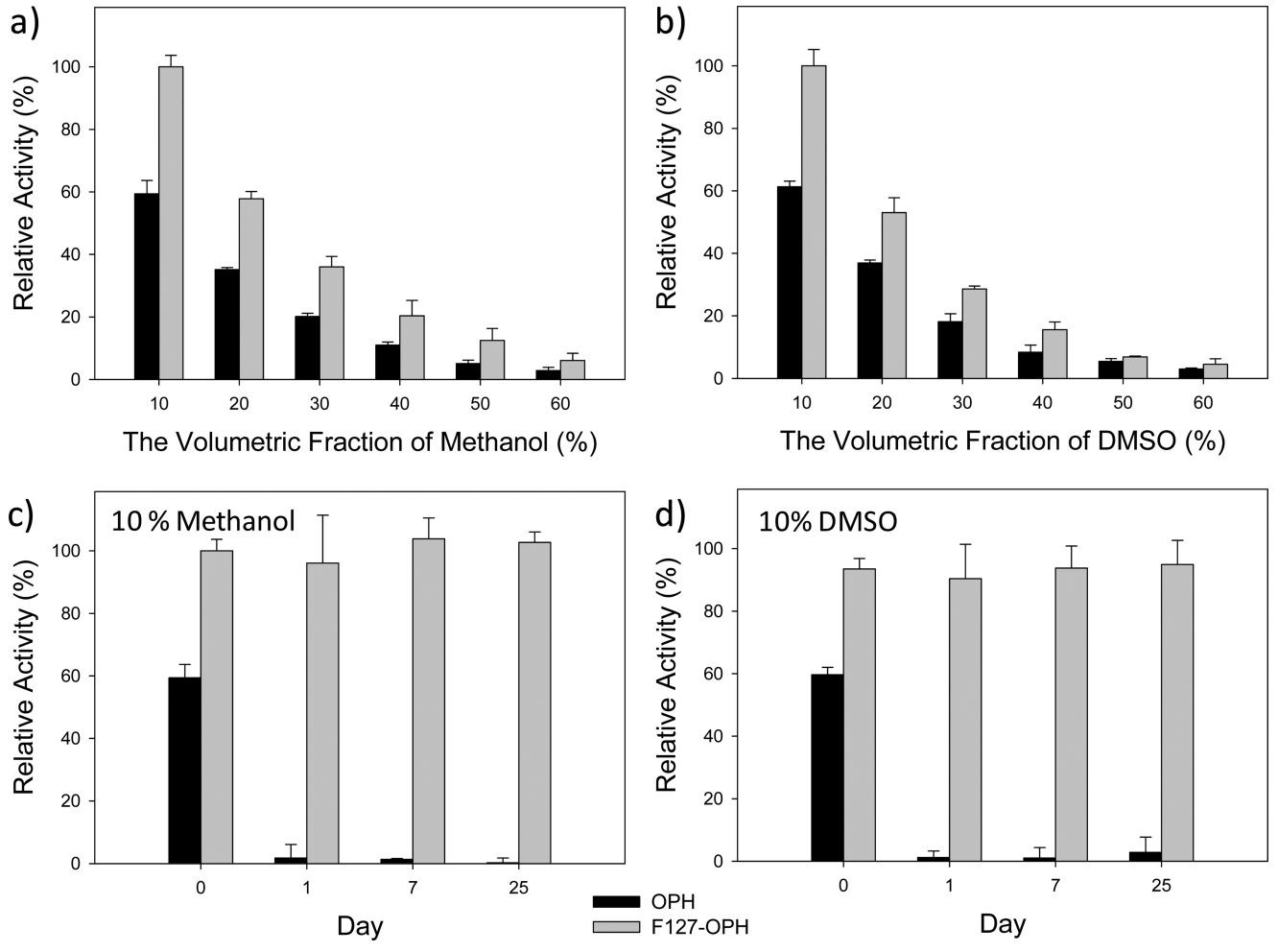


**Figure 5.** Relative activities of OPH and F127-OPH in the presence of different volumetric fraction of methanol (a) and DMSO (b). The long-term stability of the OPH and F127-OPH in the presence of 10% (v/v) methanol (c) and DMSO (d). The data were normalized to F127-OPH in HEPEs.

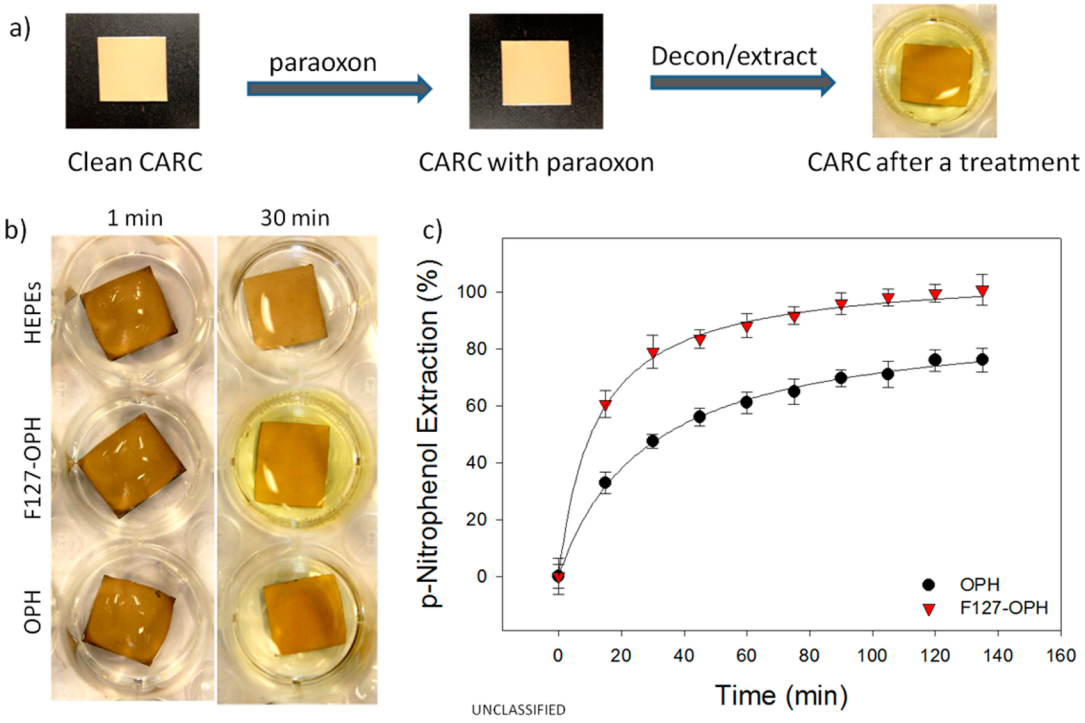


**Figure 6.** (a) Schematic representation of the decontamination procedures on the CARC surface. The yellow color is that of *p*-nitrophenol product resulting from the hydrolysis of paraoxon. (b) CARC surfaces after treating with OPH, F127-OPH, and HEPEs buffer for 30 min. (c) The decontamination and extraction efficiency of *p*-nitrophenol after a surface treatment with OPH and F127-OPH.

high decontamination efficiency observed with F127-OPH clearly suggests a great potential of using the solution of conjugate micelles as an effective decontaminant formulation.

## CONCLUSION

In summary, we have developed a facile approach to prepare robust and highly active F127-OPH conjugate micelles. The OPH in conjugate micelles exhibited reasonable improvement in activity and significantly enhanced stability, with elevated heat, multiple freeze−thaw cycles, and different substrate conditions. We believe that the F127 conjugation and the formation of micelles may provide spatial confinement to the OPH and promote a favorable OPH conformation, thereby enhancing the OPH stability. Our approach may open up a way to incorporate more functional materials onto the micelles as the enzyme activity is still preserved. As the F127-OPH conjugate micelle is fairly easy to prepare, inexpensive, nontoxic, and biodegradable, our system holds promise in the development of enzyme-based protection and decontaminant systems for military and civilian applications.

## ASSOCIATED CONTENT

### Supporting Information

Characterization of F127 and its derivatives using $^{1}$H NMR. UV−vis spectra and Lineweaver−Burk plot of the hydrolysis of paraoxon using OPH and F127-OPH. Extraction and decontamination efficiency of paraoxon using different solvents. This material is available free of charge via the Internet at http://pubs.acs.org.

## AUTHOR INFORMATION

### Corresponding Author

*Phone: 508-233-6445. Fax: 508-233-4469. E-mail: ramanathan.nagarajan.civ@mail.mil.

### Notes

The authors declare no competing financial interest.

## ACKNOWLEDGMENTS

The authors gratefully acknowledge the funding from the National Research Council, CBD Research Associateship Award, and Defense Threat Reduction Agency (DTRA). We are grateful to Dr. M. Kim (MIT), Dr. B. Olsen (MIT), and Dr. Y. Xia (Stanford) for kindly providing us the Cys 30-OPH and their helpful discussions. We thank Jason Soares and Steven Arcidiacono (NSRDEC) for help with SDS-PAGE, John Walker (NSRDEC) for help with Circular Dichroism, and David Ziegler (NSRDEC) for help with the TEM.

## REFERENCES

(1) Burnworth, M.; Rowan, S. J.; Weder, C. *Chem.—Eur. J.* **2007**, *13*, 7828−7836.
(2) Knapton, D.; Burnworth, M.; Rowan, S. J.; Weder, C. *Angew. Chem., Int. Ed.* **2006**, *45*, 5825−5829.
(3) Omburo, G. A.; Kuo, J. M.; Mullins, L. S.; Raushel, F. M. *J. Biol. Chem.* **1992**, *267*, 13278−13238.
(4) Caldwell, S. R.; Newcomb, J. R.; Schlecht, K. A.; Raushel, F. M. *Biochemistry* **1991**, *30*, 7438−7444.
(5) Dave, K. I.; Miller, C. E.; Wild, J. R. *Chem.-Biol. Interact.* **1993**, *87*, 55−68.
(6) Benning, M. M.; Kuo, J. M.; Raushel, F. M.; Holden, H. M. *Biochemistry* **1995**, *34*, 7973−7978.
(7) Yang, H.; Carr, P. D.; McLoughlin, S. Y.; Liu, J. W.; Horne, I.; Qiu, X.; Jeffries, C. M. J.; Russell, R. J.; Oakeshott, J. G.; Ollis, D. L. *Protein Eng.* **2003**, *16*, 135−145.
(8) Bigley, A. N.; Raushel, F. M. *Biochim. Biophys.* **2013**, *1834*, 443−453.
(9) Benning, M. M.; Kuo, J. M.; Raushel, F. M.; Holden, H. M. *Biochemistry* **1994**, *33*, 15001−15007.
(10) Wei, W.; Du, J. J.; Li, J.; Yan, M.; Zhu, Q.; Jin, X.; Zhu, X. Y.; Hu, Z. M.; Tang, Y.; Lu, Y. F. *Adv. Mater.* **2013**, *25*, 2212−2218.

(11) Lee, Y. W.; Stanish, I.; Rastogi, V.; Cheng, T. C.; Singh, A. *Langmuir* **2003**, *19*, 1330−1336.
(12) Pedrosa, V. A.; Paliwal, S.; Balasubramanian, S.; Nepal, D.; Davis, V.; Wild, J.; Ramanculov, E.; Simonian, A. *Colloids Surf., B* **2010**, *77*, 69−74.
(13) Chen, B. W.; Lei, C. H.; Shin, Y. S.; Liu, J. *Biochem. Biophys. Res. Commun.* **2009**, *390*, 1177−1181.
(14) Dennis, P. B.; Walker, A. Y.; Dickerson, M. B.; Kaplan, D. L.; Naik, R. R. *Biomacromolecules* **2012**, *13*, 2037−2045.
(15) Ramanathan, M.; Luckarift, H. R.; Sarsenova, A.; Wild, J. R.; Ramanculov, E. K.; Olsen, E. V.; Simonian, A. L. *Colloids Surf., B* **2009**, *73*, 58−64.
(16) Andreopoulos, F. M.; Roberts, M. J.; Bentley, M. D.; Harris, J. M.; Beckman, E. J.; Russell, A. J. *Biotechnol. Bioeng.* **1999**, *65*, 579−588.
(17) LeJeune, K. E.; Wild, J. R.; Russell, A. J. *Nature* **1998**, *395*, 27−28.
(18) LeJeune, K. E.; Russell, A. J. *Biotechnol. Bioeng.* **1999**, *62*, 659−665.
(19) Sergeeva, V. S.; Efremenko, E. N.; Kazankov, G. M.; Gladilin, A. K.; Varfolomeev, S. D. *Biotechnol. Tech.* **1999**, *13*, 479−483.
(20) Zhang, W. J.; Gilstrap, K.; Wu, L. Y.; Bahadur, K. C. R.; Moss, M. A.; Wang, Q. A.; Lu, X. B.; He, X. M. *ACS Nano* **2010**, *4*, 6747−6759.
(21) Suthiwangcharoen, N.; Nagarajan, R. *RSC Adv.* **2014**, *4*, 10076−10089.
(22) Novikov, B. N.; Grimsley, J. K.; Kern, R. J.; Wild, J. R.; Wales, M. E. *J. Controlled Release* **2010**, *146*, 318−325.
(23) Borkar, I. V.; Dinu, C. Z.; Zhu, G. Y.; Kane, R. S.; Dordick, J. S. *Biotechnol. Prog.* **2010**, *26*, 1622−1628.
(24) Suthiwangcharoen, N.; Li, T.; Li, K.; Thompson, P.; You, S. J.; Wang, Q. *Nano Res.* **2011**, *4*, 483−493.
(25) Muszanska, A. K.; Busscher, H. J.; Herrmann, A.; van der Mei, H. C.; Norde, W. *Biomaterials* **2011**, *32*, 6333−6341.
(26) Yue, Q.; Shen, T.; Wang, C.; Gao, C.; Liu, J. *Int. J. Spectrosc.* **2012**, *2012*, 1−9.
(27) Danial, M.; Klok, H. A.; Norde, W.; Stuart, M. A. C. *Langmuir* **2007**, *23*, 8003−8009.
(28) Zhang, W.; Shi, Y. A.; Chen, Y. Z.; Ye, J. A.; Sha, X. Y.; Fang, X. L. *Biomaterials* **2011**, *32*, 2894−2906.
(29) Algar, W. R.; Malonoski, A.; Deschamps, J. R.; Blanco-Canosa, J. B.; Susumu, K.; Stewart, M. H.; Johnson, B. J.; Dawson, P. E.; Medintz, I. L. *Nano Lett.* **2012**, *12*, 3793−3802.
(30) Jordan, B. J.; Hong, R.; Han, G.; Rana, S.; Rotello, V. M. *Nanotechnology* **2009**, DOI: 10.1088/0957-4484/20/43/434004.
(31) Suthiwangcharoen, N.; Li, T.; Reno, H. B.; Thompson, P.; You, S.; Wang, Q. *Biomacromolecules* **2014**, DOI: 10.1021/bm401819x.
(32) Gulla, K. C.; Gouda, M. D.; Thakur, M. S.; Karanth, N. G. *Biosens. Bioelectron.* **2004**, *19*, 621−625.
(33) Gouda, M. D.; Singh, S. A.; Rao, A. G.; Thakur, M. S.; Karanth, N. G. *J. Biol. Chem.* **2003**, *278*, 24324−24333.
(34) Khmelnitsky, Y. L.; Belova, A. B.; Levashov, A. V.; Mozhaev, V. V. *FEBS Lett.* **1991**, *284*, 267−269.